Nanoscale

Controlling optical polarization conversion with $Ge_2Sb_2Te_5$-based phase-change dielectric metamaterials

Journal:	*Nanoscale*
Manuscript ID	NR-ART-03-2018-002587.R1
Article Type:	Paper
Date Submitted by the Author:	05-May-2018

Complete List of Authors:	Zhu, Wei; Northwestern Polytechnical University Yang, Ruisheng; Northwestern Polytechnical University Fan, Yuancheng; Northwestern Polytechnical University, Department of Applied Physics, School of Science Fu, Quanhong; Key Laboratory of Space Applied Physics and Chemistry, Ministry of Education and Department of Applied Physics, School of Science, Northwestern Polytechnical University Wu, Hongjing; Northwestern Polytechnical University, Department of Applied Physics Zhang, Peng; Ames Laboratory; Iowa State University Shen, Nian-Hai; Ames Laboratory; Iowa State University Zhang, Fuli; Key Laboratory of Space Applied Physics and Chemistry, Ministry of Education and Department of Applied Physics, School of Science, Northwestern Polytechnical University,

Nanoscale

ARTICLE

Controlling optical polarization conversion with $Ge_2Sb_2Te_5$-based phase-change dielectric metamaterials

Received 00th January 20xx,
Accepted 00th January 20xx

DOI: 10.1039/x0xx00000x

www.rsc.org/nanoscale

Wei Zhu,†[a] Ruisheng Yang,†[a] Yuancheng Fan,*[a] Quanhong Fu,[a] Hongjing Wu,[a] Peng Zhang,[b] Nian-Hai Shen[b] and Fuli Zhang*[a]

Recent progress on metamaterial based polarization manipulation of light is promising for novel polarization dependent optical components or systems. To go beyond the limited frequency bandwidth of metamaterial that due to its resonant nature, it is highly desirable to incorporate tunability into metamaterial-based polarization manipulations. Here, we propose a dielectric metamaterial for controlling the linear polarization conversion using the phase-change characteristic of $Ge_2Sb_2Te_5$ (GST), whose refractive index changes significantly when transfoming from the amorphous phase to the crystalline phase under external stimulus. The polarization conversion phenomena are systematically studied by different arrangement of GST in this metamaterial. The performance of linear polarization conversion and the tunability are also analyzed and compared in three different designs. It is found that the phase-change materials such as GST can be employed in dielectric material for tunable and switchable linear polarization conversion in the telecom band. The conversion efficiency can be significantly modulated during the phase transition. Our results provide useful insights of incorparating phase-change materials with metamaterials for the tunable polarization manipulation.

Introduction

Metamaterials,[1-3] a kind of artificial materials with exotic properties beyond natural media, have attracted considerable attention in realizing novel functions in optical components or systems.[4] Since the first experimental demonstration of negative refraction with periodic metallic wires and split ring resonators at the microwave frequency,[5] more and more novel electromagnetic phenomena and extraordinary applications have been inspired ranging from microwave to visible frequencies,[6-33] such as invisibility cloaking,[6-15] perfect absorbers,[16-21] high resolution lenses,[22, 23] and polarization manipulation.[24-31]

While metallic metamaterials are restricted in performance by the ohmic damping when reaching near the optical frequency, dielectric metamaterials with their building blocks made of low-loss dielectrics,[34-38] are raised to resolve the loss issue, by exhibiting a certain order of Mie resonance other than conducting currents in its sub-atoms. In addition, considering most metamaterials can usually only work within a specific narrow frequency band due to their local resonant nature which limits the application in reality. For improving the performance, some studies have been focused on tunable metamaterials by incorporating tunable mechanism within the subwavelength unit cells of metamaterials, these including the introducing of semiconductors,[39-46] lumped elements,[47-51] liquid crystals,[52-57] ferromagnetic and ferroelectric materials,[58, 59] and grapheme.[60-72]

Phase-change material $Ge_2Sb_2Te_5$ (GST)[73-77] has emerged as a promising candidate for manipulating optical waves, because its optical and electrical properties can be changed drastically from amorphous (a-GST) to crystalline state (c-GST)[78-80] by applying either heat, photonic, or electric power on it. More interestingly, GST has both phases stable at the room temperature and can be quickly and reversibly switched between one and the other without volatilization at a time scale of 50 ns,[81] and an arbitrary intermediate crystalline state between a-GST and c-GST can be stably stayed by precisely controlling the energy and duration of the stimulus.[80] The different bonding mechanisms for these two phases, i.e., covalent bonding for the amorphous phase and metavalent bonding for the crystalline phase, will lead to different dielectric functions in optical frequencies.[82] In this way, optical waves can be modulated by exploiting the large contrast ratio on complex refractive index between a-GST and c-GST phases.[79] The different optical response can be further employed for designing phase change metamaterials with switchable manipulations on light.

In this article, we proposed dielectric metamaterials with tunability and high optical polarization conversion efficiency (PCE) based on $Ge_2Sb_2Te_5$. We systematically studied the behaviour of GST metamaterials with different geometric sizes, crystallization ratio and incident angles, numerically compared

[a] Key Laboratory of Space Applied Physics and Chemistry, Ministry of Education and Department of Applied Physics, School of Science, Northwestern Polytechnical University, Xi'an 710129, China. Email: phyfan@nwpu.edu.cn; fuli.zhang@nwpu.edu.cn
[b] Ames Laboratory and Department of Physics and Astronomy, Iowa State University, Ames, Iowa 50011, United States
† These authors contributed equally to this work.

the linear polarization converter (LPC) performance of three different designs, and explored the tunability of complex refractive index benefitting from its phase-change feature. We found that all structures with a-GST show high polarization conversion ratio (PCR).

Results and discussion

Figure 1 shows schematically the proposed dielectric metamaterial as the linear polarization converter. The metamaterial is composed of an array of L-shaped dielectric resonators, and a silver ground plane, with a low index glass spacer. For a systemically investigation of the controllable polarization conversion behaviour, we study structures with three variations as controlled groups, where GST (yellow in Fig. 1) was set as different parts of the dielectric metamaterial: (i) GST film is sandwiched in between the silver ground plane and a layer of glass, with L-shaped silicon resonators placed on top of the glass as shown in Fig. 1c; (ii) GST film is coated on top of the L-shaped silicon resonators as shown in Fig. 1d; (iii) GST film is constructed as the top L-shaped resonators as shown in Fig. 1e. The light is incident on the top surface of the dielectric metamaterial polarized along x/y-axis (in considering the oblique case). The bottom of the LPC is a fully reflective silver ground plane in order to totally suppress the wave transmission, assisting high efficient control of light in reflection mode. In the study, the low-index glass is modelled by n= 1.48, and the dispersive index of refraction n and extinction coefficient k of GST films are plotted for both amorphous and crystalline states (a-GST and c-GST) in Fig. 1b.[79] We can see that the refractive index of GST changes smoothly in the telecommunication wavelength band. Note that the extinction coefficient of GST representing the absorbing ability is negligible in the amorphous state while relatively large in the crystalline state in the highlight region (λ~1.55μm), indicating that the GST will be a good candidate in realizing high-efficiency and tunable metamaterials with predesigned functions in the telecom band, such as in depth polarization modulation.

The low-loss of amorphous state and high contrast ratio in refraction index and extinction coefficient are beneficial for achieving high modulation depth in polarization conversion in telecom band. We employed a finite-difference-time-domain (FDTD) method based electromagnetic solver for investigating the polarization conversion properties of the proposed metamaterials. In the simulations, periodic boundary conditions were set along the x and y directions to simulate an infinite periodic array, and a plane wave was incident on the top surface of the proposed designs with *y*-polarized electric field ($\mathbf{E}_{yi}=E_{yi}\mathbf{e}_y$).

In our analysis, we calculated the complex reflection coefficients for both cross-polarized and co-polarized light. Since the phase of GST can be controlled by precisely controlling the external stimulus, GST film can be with arbitrary hybridization ratio of a-GST and c-GST, and thus the efficiency of LPCs can be gradually tuned. Among the several effective-medium theories developed for the description of the optical constants/dielectric functions of heterogeneous medium, Lorentz-Lorenz relation is one of the best candidates and has been successfully applied in the GST thin film in different crystallization ratio. The optical constants of GST with a certain hybridization ratio of a-GST and c-GST can be calculated using the Lorenz-Lorentz relations,[83]

$$\frac{\varepsilon_{eff}(\lambda)-1}{\varepsilon_{eff}(\lambda)+2}=\eta\times\frac{\varepsilon_{CGST}(\lambda)-1}{\varepsilon_{CGST}(\lambda)+2}+(1-\eta)\times\frac{\varepsilon_{AGST}(\lambda)-1}{\varepsilon_{AGST}(\lambda)+2}.$$

where $\varepsilon_{CGST}(\lambda)$ and $\varepsilon_{AGST}(\lambda)$ are wavelength-dependent dielectric constants of GST in crystalline and amorphous states, and η is the crystallization fraction of GST ranging from 0 (pure a-GST) to 1 (pure c-GST). Results are shown in Fig. 2.

In the study, we mainly explored the mechanism of the GST in the tunable LPC for the three different structures via changing arrangement of GST. Obviously, the PCE obtained by our LPCs is varied by the characteristics of GST. As the ground plane of the LPC blocks light from passing through the metamaterial and we fix the incident polarized in y-direction,

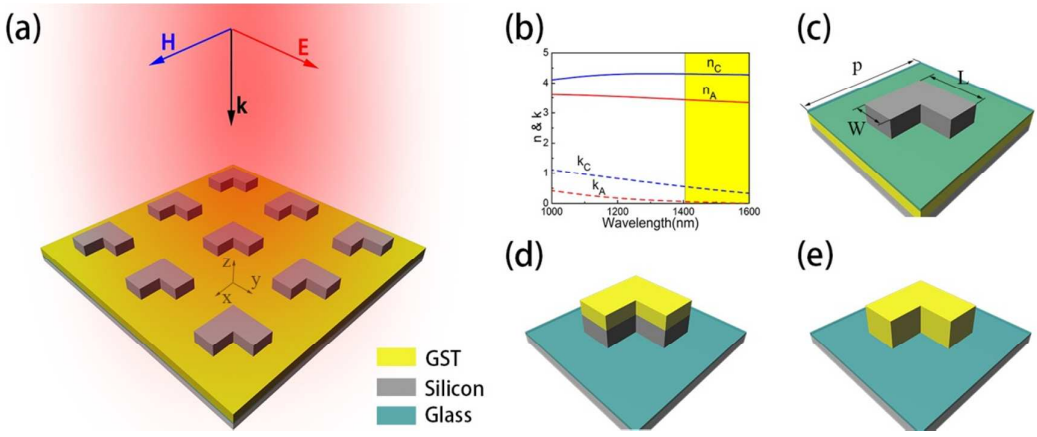

Fig. 1 (a) Schematic of the proposed dielectric metamaterials consisting of periodically arranged L-shaped resonators. (b) Index of refraction n and extinction coefficient k of amorphous (subscript A) and crystalline (subscript C) GST. (c)-(e) Different structures of the dielectric metamaterial containing GST: The GST film serves as dielectric spacer, covering on the silicon resonator, and the L-shaped resonator, respectively.

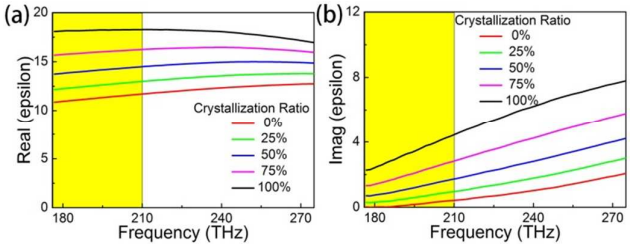

Fig. 2 The (a) real and (b) imaginary part of the permittivity of GST with different crystallization ratio.

the scattered light with different polarizations can be well defined by the $R_{yy}=(E_{yr}/E_{yi})^2$ and $R_{xy}=PCE=(E_{xr}/E_{yi})^2$ representing the co-polarization (y-to-y) and cross-polarization (y-to-x) reflection, respectively. The subscript i and r represent the incident and reflected light. To evaluate the performance of the polarization converters quantitatively, we define the PCR as:

$$PCR = |R_{xy}|/(|R_{yy}| + |R_{xy}|).$$

First, we explore the polarization conversion in the dielectric metamaterial with GST substrate (see Fig. 1c). The periodic array of L-shaped resonators are made of silicon, the lattice constant is p=1000 nm, the length and width are l=700 nm and w=320 nm, the thickness of the resonator is 300 nm. The dielectric spacer is stacked GST layer and low-index glass layer with thicknesses of 65 nm and 75 nm, respectively. The reflection spectra with 65 nm-thick a-GST are shown in Fig. 3b. where there is one dip of R_{xy} around 182 THz indicating that no polarization conversion happens, and the other dip of R_{yy} around 188 THz with R_{xy}=77.3%, implying a high polarization conversion.

The magnetic field distribution of the resonant mode at 188 THz is also plotted in the inset of Fig. 3b. Since it oscillates along the L-shaped resonator, the x- and y- components of the mode can couple to both the x- and y-polarized light, leading to the polarization conversion around the resonant frequency. It is

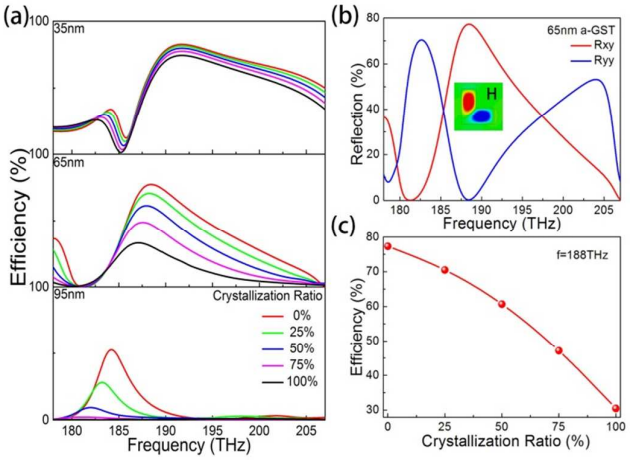

Fig. 3 (a) PCE of the dielectric metamaterial LPC with GST of different thickness and crystallization ratio. (b) Reflection spectra for x (red)/y (blue) polarizations of LPC with a 65 nm-thick a-GST substrate under the y-polarized illumination. The H field distribution at R_{xy} peak (188 THz) is shown as insets. (c) Modulation on the PCE by crystallization ratio with a 65 nm-thick substrate at 188 THz.

also worth noting that the two resonances are promising for realizing a broadband or dual-band cross-polarization converter via geometric optimization.

The advantages of the GST-based LPC are of its tunable side by exploiting a partial crystalline state between a-GST and c-GST and the geometric dimension of the GST film. Figure 3a shows that the PCE strongly depends on the crystallization ratio (ranging from 0% to 100%) and GST film thickness (ranging from 35 nm to 95 nm). As can be seen, the PCE can be greatly modulated by designing the geometry of the dielectric metamaterial or by changing the crystallization ratio of GST. The maximum PCE maintains the highest value of 82.7% near 192 THz when the thickness of a-GST is 35nm, while the efficiency drops to the relatively highest value of 52.5% near 184 THz with the thickness of a-GST increasing to 95 nm. Furthermore, we notice that the bandwidth of the LPCs also undertakes a dramatic change. Obviously, broadband polarization conversion can be realized from 187 THz to 207 THz when the thickness of GST is 35 nm no matter what the crystallization ratio of GST is. The modulation on the PCE is more effective but the conversion efficiency is lower with thicker GST films, resulting from the higher absorption in bulk GST materials. In order to compromise the PCE and the tunability of our device, we choose the GST film thickness to be 65 nm as a trade-off point.

Figure 4a, d, and g show the calculated PCR for structures shown in Fig. 1c. As in Fig. 4a, the PCR is higher than 99.9% at the resonant frequency, indicating nearly total polarization conversion. The PCR keeps a high value from 185 THz to 207 THz, which implies the broadband feature of the proposed LPC with a 35 nm-thick GST film. The decrease of the PCR spectra peaks is negligible with different GST thickness. For the 65 nm-thick a-GST, the PCR peak value is 99.7%, while for the 95 nm-thick a-GST, it is 94.4%. The PCE of the LPC under oblique incidence was also explored. The x- and y-polarized PCE as function of incident angles and incident frequencies are shown in Fig. 4b, e and h and Fig. 4c, f and i, respectively. Near the resonant frequency, LPCs have relatively high PCE when the incident angle is within from 0° to 15°.

Then we consider the case in which the GST film is coated on top of the L-shaped silicon resonators as shown in Fig. 1d. The two layers of the L-shaped resonator are 200 nm-thick Silicon and 130 nm-thcik GST on top, and the width of the L-shaped resonator is w=330 nm. The thickness of the glass is 75 nm. The reason for the slightly different geometrical parameters is that GST acting as part of the resonant unit is directly coupled to optical waves. This setup can improve the sensitivity of the modulation, and in addition, the phase of GST can be completely, quickly and reversibly changed by external pumping light. There exist two resonant dips at 183 THz and 192 THz on the co-polarization reflection spectrum as shown in Fig. 5a. It is obvious that the LPC with a-GST as the covering layer has realized the broadband polarization conversion. The PCE is over 60% from 188 THz to 201 THz. As the inset of Fig. 5a shows, the distribution of the **H** field at the peak frequency of cross-polarization is plotted. The **H** field is on the centre of the two arms (Field distribution revise). Note that the GST layer plays important roles for this covering layer since it not only combining with silicon so as to increase the PCE, but also realizing the tunable ability through phase transitions of GST under

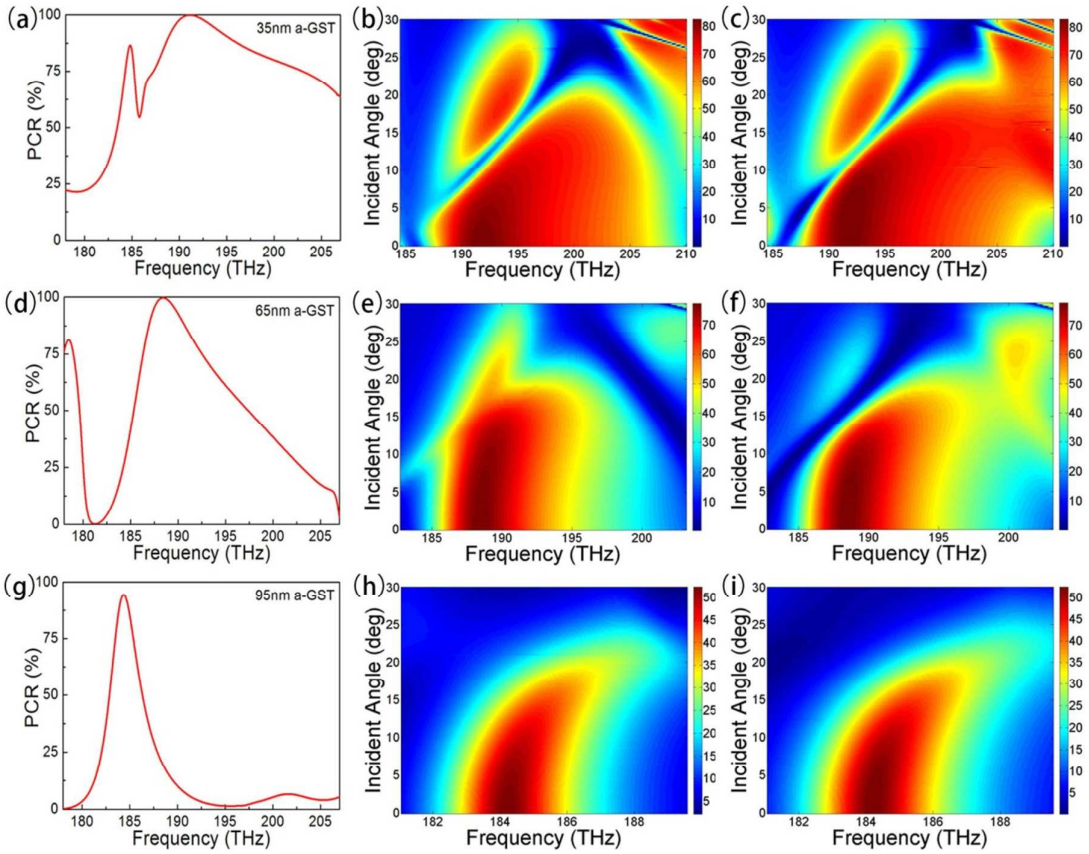

Fig. 4 PCR and PCE maps for a-GST substrate with different thickness as (a)~(c) 35 nm, (d)~(h) 65 nm and (g)~(i) 95 nm, and PCE maps with angle of incidence from 0°to 30° of (b), (e), (h) TE transfer TM and (c), (f), (i) TM transfer TE.

external stimulus.

Since GST is a part of the L-shaped dielectric resonator in this case, the geometrical parameters must be redesigned in order to maintain a high PCE and broad operating bandwidth. We made an optimization and researched the relationship between the crystallization ratio of GST and the PCE as shown in Fig. 5b. The PCE is over 60% from 188 THz to 201 THz with a-GST, while significantly decreases due to the increased absorption with the phase transition of the GST from amorphous to crystalline. Figure 5c proves the tunability of PCE, which changes from 75.2% to 9.5% at 192 THz under a phase transition from pure a-GST to pure c-GST. In comparison to the first case where GST is embedded in the substrate, setting GST as the cover on the silicon resonator offers a wider operating band and larger modulation depth. Besides, the resonant frequency has a redshift with the increase of the GST crystallization ratio owing to the increasing of refractive index. We note that this structure can also realize the broadband PCR as shown in Fig. 5d. The PCR is above 80% from 187 THz to 203 THz, and reaches 99.8% representing the maximum cross-polarization and the minimum co-polarization at 192 THz. We also studied the PCE map with different incident angles from 0° to 30° for both the TE and TM polarizations as shown in Fig. 6. The broadband PCE maintains at relative lager incident angle especially for the TE case.

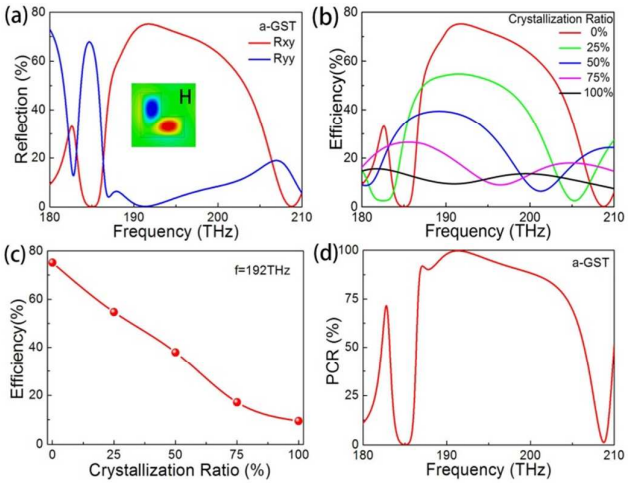

Fig. 5 (a) Reflection spectra of the LPC with the GST as covering layer. (the H field distribution at R_{xy} peak (192 THz) for the structure is shown insets) (b) PCE with different crystallization ratio with GST covering layer. (c) Modulation on the PCE of crystallization ratio at 192 THz. (d) PCR of the LPC for the a-GST as covering layer.

Finally, we also explore an extreme case where the top resonator is made of GST as shown in Fig. 1e. The thickness of the GST resonator is 400 nm, the width w is 350 nm, and the thickness of the glass spacer is 80 nm. The geometric parame-

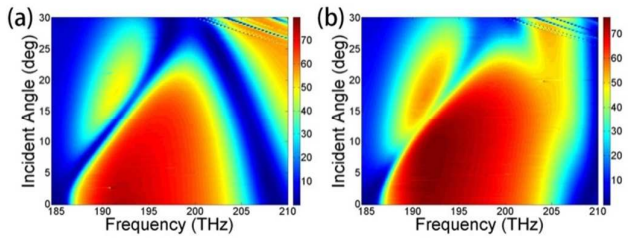

Fig. 6 PCE map for a-GST as covering layer with different incident angles from 0°to 30° of (a) TE transfer TM and (b) TM transfer TE.

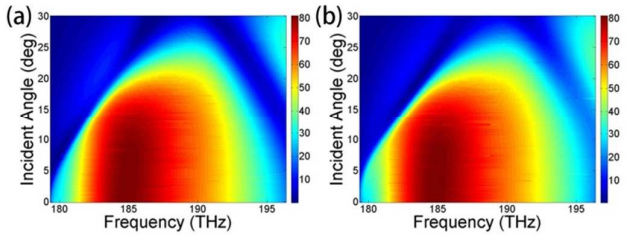

Fig. 8 PCE map for a-GST as resonator with different incident angles from 0°to 30° of (a) TE transfer TM and (b) TM transfer TE.

ters of the structure have changed a bit to settle the feature frequency since the permittivity of the GST is different from silicon. There also exist two peaks of R_{xy} locating at 185 THz and 202 THz, respectively. The second peak is weak due to the relatively strong absorption around this frequency of a-GST. In contrary, GST has little absorption at the first resonant frequency, which leads to the high PCE. The distributions of magnetic field at 185 THz are shown in the inset. As the phase of EM wave changes, the distribution of magnetic field changes rapidly between the corner of the L-shaped resonator and the two arms of the resonator.

The metamaterial with pure a-GST has a peak PCE at 185 THz as can be seen from Fig. 7b, and the PCE decreases at the resonant frequency with the mixing of c-GST. It is also observed that when the resonator is fully composed of GST, the LPC is more sensitive to the dielectric loss. A slight phase change of GST would cause a dramatic change in the efficiency of polarization conversion because the LPC is highly dependent on the resonant strength, and the strength of resonance is sensitive to the dielectric loss in the resonator. Figure 7c shows that the PCE can realize a modulation from 80.6% to 1.9% at 185 THz with crystallization ratio ranging from 0% to 100%. It is clear that the performance of this LPC is mainly determined by GST. The PCE of this configuration reaches the highest value among the three LPCs of 80.6% at 185 THz. In addition,

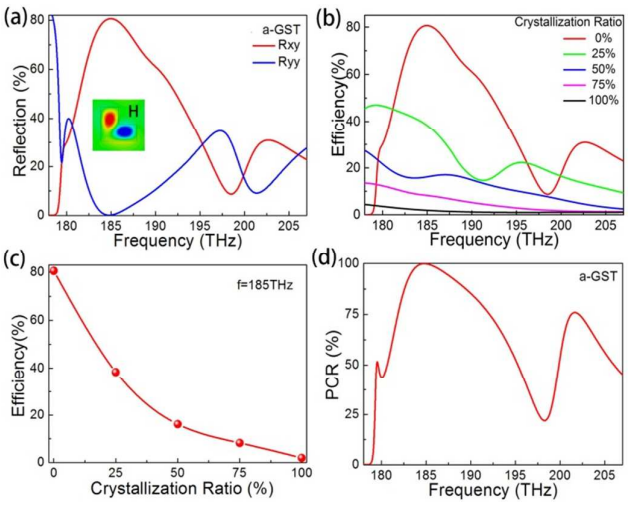

Fig. 7 (a) Reflection spectra for the LPC with the a-GST as the resonator. (the H field distribution at reflection dips for the structure is shown insets) (b) PCE with the different crystallization ratio of GST. (c) Modulation on the PCE of crystallization ratio at 185THz. (d) PCR of the LPC for the a-GST as the resonator.

at 185 THz and 202 THz, the PCR of a-GST reaches 99.9% and 75.9%, respectively as shown in Fig. 7d. We also calculate the PCE map with different incident angles from 0°to 30° and results are shown in Fig. 8. The PCE maintains a high value (higher than 60%) when the angle of incident wave varies from 0° to 15°. Comparing to the previous two LPCs, we found that the modulation depth will be significantly improved if the resonator is completely composed of GST due to larger absorption and the resonant peaks will undertake a redshift if GST stands from amorphous to the crystalline state. In this case, the thickness of the GST which offers the capacity of tunable PCE is much thicker than previous two models.

Conclusion

In summary, we demonstrated that the phase-change material GST can be incorporated in dielectric materials to achieve tunable and switchable linear polarization conversion in the telecom band. Metamaterials with different arrangement of GST in the structure are systematically studied. We have also demonstrated three tunable reflective LPCs based on the GST phase-change material in telecom band. These LPCs all showed high PCE and PCR with a-GST (PCR＞99.7%). The maximum PCE is about 80%, it is mainly limited by the loss in GST films. The metamaterial structure can be further optimized to achieve improved PCE. The proposed tunable LPCs offer superior properties and performance compared to the conventional LPCs known to be inherently inefficient and untunable. The mechanism of the tunability employing phase-change material can be extended to various polarization manipulation based applications.

Conflicts of interest

There are no conflicts to declare.

Acknowledgements

The authors would like to acknowledge financial support from the National Science Foundation of China (NSFC) (Grants Nos. 61771402, 61505164, 11674266, 11372248, 51575297), the Fundamental Research Funds for the Central Universities (Grant No. 3102017zy033), and the Natural Science Basic Research Plan in Shaanxi Province of China (Program No. 2017JM6094). Work at Ames Laboratory was partially

supported by the U.S. Department of Energy, Office of Basic Energy Science, Division of Materials Science and Engineering (Ames Laboratory is operated for the U.S. Department of Energy by Iowa State University under Contract No. DE-AC02-07CH11358).

Notes and references

1. D. R. Smith, J. B. Pendry and M. C. K. Wiltshire, *Science*, 2004, **305**, 788-792.
2. V. M. Shalaev, *Nature Photonics*, 2007, **1**, 41-48.
3. C. M. Soukoulis and M. Wegener, *Nature Photonics*, 2011, **5**, 523-530.
4. N. I. Zheludev and Y. S. Kivshar, *Nature Materials*, 2012, **11**, 917-924.
5. R. A. Shelby, D. R. Smith and S. Schultz, *Science*, 2001, **292**, 77-79.
6. D. Schurig, J. J. Mock, B. J. Justice, S. A. Cummer, J. B. Pendry, A. F. Starr and D. R. Smith, *Science*, 2006, **314**, 977-980.
7. W. S. Cai, U. K. Chettiar, A. V. Kildishev and V. M. Shalaev, *Nature Photonics*, 2007, **1**, 224-227.
8. J. S. Li and J. B. Pendry, *Physical Review Letters*, 2008, **101**, 203901.
9. R. Liu, C. Ji, J. J. Mock, J. Y. Chin, T. J. Cui and D. R. Smith, *Science*, 2009, **323**, 366-369.
10. J. Valentine, J. S. Li, T. Zentgraf, G. Bartal and X. Zhang, *Nature Materials*, 2009, **8**, 568-571.
11. L. H. Gabrielli, J. Cardenas, C. B. Poitras and M. Lipson, *Nature Photonics*, 2009, **3**, 461-463.
12. T. Ergin, N. Stenger, P. Brenner, J. B. Pendry and M. Wegener, *Science*, 2010, **328**, 337-339.
13. T. C. Han, X. Bai, D. L. Gao, J. T. L. Thong, B. W. Li and C. W. Qiu, *Physical Review Letters*, 2014, **112**, 054302.
14. X. J. Ni, Z. J. Wong, M. Mrejen, Y. Wang and X. Zhang, *Science*, 2015, **349**, 1310-1314.
15. R. G. Peng, Z. Q. Xiao, Q. Zhao, F. L. Zhang, Y. G. Meng, B. Li, J. Zhou, Y. C. Fan, P. Zhang, N. H. Shen, T. Koschny and C. M. Soukoulis, *Physical Review X*, 2017, **7**, 011033.
16. N. I. Landy, S. Sajuyigbe, J. J. Mock, D. R. Smith and W. J. Padilla, *Physical Review Letters*, 2008, **100**, 207402.
17. N. Liu, M. Mesch, T. Weiss, M. Hentschel and H. Giessen, *Nano Letters*, 2010, **10**, 2342-2348.
18. J. M. Hao, J. Wang, X. L. Liu, W. J. Padilla, L. Zhou and M. Qiu, *Applied Physics Letters*, 2010, **96**, 251104.
19. J. F. Zhang, K. F. MacDonald and N. I. Zheludev, *Light-Sci Appl*, 2012, **1**, e18.
20. Y. C. Fan, Z. Liu, F. L. Zhang, Q. Zhao, Z. Y. Wei, Q. H. Fu, J. J. Li, C. Z. Gu and H. Q. Li, *Scientific Reports*, 2015, **5**, 13956.
21. F. L. Zhang, S. Q. Feng, K. P. Qiu, Z. J. Liu, Y. C. Fan, W. H. Zhang, Q. Zhao and J. Zhou, *Applied Physics Letters*, 2015, **106**, 091907.
22. A. Grbic and G. V. Eleftheriades, *Physical Review Letters*, 2004, **92**, 117403.
23. Z. W. Liu, H. Lee, Y. Xiong, C. Sun and X. Zhang, *Science*, 2007, **315**, 1686-1686.
24. J. M. Hao, Y. Yuan, L. X. Ran, T. Jiang, J. A. Kong, C. T. Chan and L. Zhou, *Physical Review Letters*, 2007, **99**, 063908.
25. J. K. Gansel, M. Thiel, M. S. Rill, M. Decker, K. Bade, V. Saile, G. von Freymann, S. Linden and M. Wegener, *Science*, 2009, **325**, 1513-1515.
26. C. Menzel, C. Helgert, C. Rockstuhl, E. B. Kley, A. Tunnermann, T. Pertsch and F. Lederer, *Physical Review Letters*, 2010, **104**, 253902.
27. N. I. Zheludev, E. Plum and V. A. Fedotov, *Applied Physics Letters*, 2011, **99**, 171915.
28. J. Han, H. Q. Li, Y. C. Fan, Z. Y. Wei, C. Wu, Y. Cao, X. Yu, F. Li and Z. S. Wang, *Applied Physics Letters*, 2011, **98**, 151908.
29. Z. Y. Wei, Y. Cao, Y. C. Fan, X. Yu and H. Q. Li, *Applied Physics Letters*, 2011, **99**, 221907.
30. M. Mutlu, A. E. Akosman, A. E. Serebryannikov and E. Ozbay, *Physical Review Letters*, 2012, **108**, 213905.
31. Y. F. Li, J. Q. Zhang, H. Ma, J. F. Wang, Y. Q. Pang, D. Y. Feng, Z. Xu and S. B. Qu, *Scientific Reports*, 2016, **6**, 34518.
32. Y. Fan, F. Zhang, N.-H. Shen, Q. Fu, Z. Wei, H. Li and C. M. Soukoulis, *Phys. Rev. A*, 2018, **97**, 003800.
33. N. H. Shen, P. Zhang, T. Koschny and C. M. Soukoulis, *Physical Review B*, 2016, **93**, 245118.
34. Q. Zhao, J. Zhou, F. L. Zhang and D. Lippens, *Mater Today*, 2009, **12**, 60-69.
35. J. C. Ginn, I. Brener, D. W. Peters, J. R. Wendt, J. O. Stevens, P. F. Hines, L. I. Basilio, L. K. Warne, J. F. Ihlefeld, P. G. Clem and M. B. Sinclair, *Physical Review Letters*, 2012, **108**, 097402.
36. P. Moitra, Y. M. Yang, Z. Anderson, I. I. Kravchenko, D. P. Briggs and J. Valentine, *Nature Photonics*, 2013, **7**, 791-795.
37. S. Jahani and Z. Jacob, *Nat Nanotechnol*, 2016, **11**, 23-36.
38. Q. Zhao, Z. Q. Xiao, F. L. Zhang, J. M. Ma, M. Qiao, Y. G. Meng, C. W. Lan, B. Li, J. Zhou, P. Zhang, N. H. Shen, T. Koschny and C. M. Soukoulis, *Advanced Materials*, 2015, **27**, 6187-6194.
39. Q. F. Xu, B. Schmidt, S. Pradhan and M. Lipson, *Nature*, 2005, **435**, 325-327.
40. H. T. Chen, W. J. Padilla, J. M. O. Zide, A. C. Gossard, A. J. Taylor and R. D. Averitt, *Nature*, 2006, **444**, 597-600.
41. H. T. Chen, J. F. O'Hara, A. K. Azad, A. J. Taylor, R. D. Averitt, D. B. Shrekenhamer and W. J. Padilla, *Nature Photonics*, 2008, **2**, 295-298.
42. H. T. Chen, W. J. Padilla, M. J. Cich, A. K. Azad, R. D. Averitt and A. J. Taylor, *Nature Photonics*, 2009, **3**, 148-151.
43. P. R. West, S. Ishii, G. V. Naik, N. K. Emani, V. M. Shalaev and A. Boltasseva, *Laser & Photonics Reviews*, 2010, **4**, 795-808.
44. J. Q. Gu, R. Singh, X. J. Liu, X. Q. Zhang, Y. F. Ma, S. Zhang, S. A. Maier, Z. Tian, A. K. Azad, H. T. Chen, A. J. Taylor, J. G. Han and W. L. Zhang, *Nature Communications*, 2012, **3**, 1151.
45. S. Zhang, J. F. Zhou, Y. S. Park, J. Rho, R. Singh, S. Nam, A. K. Azad, H. T. Chen, X. B. Yin, A. J. Taylor and X. Zhang, *Nature Communications*, 2012, **3**, 942.
46. N. H. Shen, M. Massaouti, M. Gokkavas, J. M. Manceau, E. Ozbay, M. Kafesaki, T. Koschny, S. Tzortzakis and C. M. Soukoulis, *Physical Review Letters*, 2011, **106**, 037403.
47. I. V. Shadrivov, S. K. Morrison and Y. S. Kivshar, *Optics Express*, 2006, **14**, 9344-9349.
48. Y. C. Fan, J. Han, Z. Y. Wei, C. Wu, Y. Cao, X. Yu and H. Q. Li, *Applied Physics Letters*, 2011, **98**, 151903.
49. Q. H. Fu, F. L. Zhang, Y. C. Fan, X. He, T. Qiao and B. T. Kong, *Optics Express*, 2016, **24**, 1708-1715.
50. Y. C. Fan, T. Qiao, F. L. Zhang, Q. H. Fu, J. J. Dong, B. T. Kong and H. Q. Li, *Scientific Reports*, 2017, **7**, 40441.
51. Q. H. Fu, F. L. Zhang, Y. C. Fan, J. J. Dong, W. Q. Cai, W. Zhu, S. A. Chen and R. S. Yang, *Applied Physics Letters*, 2017, **110**, 221905.
52. X. Wang, D. H. Kwon, D. H. Werner, I. C. Khoo, A. V. Kildishev and V. M. Shalaev, *Applied Physics Letters*, 2007, **91**, 143122.
53. Q. Zhao, L. Kang, B. Du, B. Li, J. Zhou, H. Tang, X. Liang and B. Z. Zhang, *Applied Physics Letters*, 2007, **90**, 011112.
54. W. Dickson, G. A. Wurtz, P. R. Evans, R. J. Pollard and A. V. Zayats, *Nano Letters*, 2008, **8**, 281-286.
55. F. Zhang, Q. Zhao, L. Kang, D. P. Gaillot, X. P. Zhao, J. Zhou and D. Lippens, *Applied Physics Letters*, 2008, **92**, 193104.

56. C. L. Chang, W. C. Wang, H. R. Lin, F. J. Hsieh, Y. B. Pun and C. H. Chan, *Applied Physics Letters*, 2013, **102**, 151903.
57. D. Shrekenhamer, W. C. Chen and W. J. Padilla, *Physical Review Letters*, 2013, **110**, 177403.
58. L. Kang, Q. Zhao, H. J. Zhao and J. Zhou, *Optics Express*, 2008, **16**, 8825-8834.
59. Q. Zhao, B. Du, L. Kang, H. J. Zhao, Q. Xie, B. Li, X. Zhang, J. Zhou, L. T. Li and Y. G. Meng, *Applied Physics Letters*, 2008, **92**, 051106.
60. L. Ju, B. S. Geng, J. Horng, C. Girit, M. Martin, Z. Hao, H. A. Bechtel, X. G. Liang, A. Zettl, Y. R. Shen and F. Wang, *Nat Nanotechnol*, 2011, **6**, 630-634.
61. T. Low and P. Avouris, *Acs Nano*, 2014, **8**, 1086-1101.
62. T. Low, A. Chaves, J. D. Caldwell, A. Kumar, N. X. Fang, P. Avouris, T. F. Heinz, F. Guinea, L. Martin-Moreno and F. Koppens, *Nature Materials*, 2017, **16**, 182-194.
63. P. Tassin, T. Koschny and C. M. Soukoulis, *Science*, 2013, **341**, 620-621.
64. Z. Y. Fang, Y. M. Wang, A. E. Schather, Z. Liu, P. M. Ajayan, F. J. G. de Abajo, P. Nordlander, X. Zhu and N. J. Halas, *Nano Letters*, 2014, **14**, 299-304.
65. Y. C. Fan, F. L. Zhang, Q. Zhao, Z. Y. Wei and H. Q. Li, *Opt Lett*, 2014, **39**, 6269-6272.
66. H. Cheng, S. Q. Chen, P. Yu, W. W. Liu, Z. C. Li, J. X. Li, B. Y. Xie and J. G. Tian, *Advanced Optical Materials*, 2015, **3**, 1744-1749.
67. M. S. Jang, V. W. Brar, M. C. Sherrott, J. J. Lopez, L. Kim, S. Kim, M. Choi and H. A. Atwater, *Physical Review B*, 2014, **90**, 165409.
68. Y. C. Fan, N. H. Shen, T. Koschny and C. M. Soukoulis, *Acs Photonics*, 2015, **2**, 151-156.
69. P. A. Huidobro, M. Kraft, S. A. Maier and J. B. Pendry, *Acs Nano*, 2016, **10**, 5499-5506.
70. Y. C. Fan, N. H. Shen, F. L. Zhang, Z. Y. Wei, H. Q. Li, Q. Zhao, Q. H. Fu, P. Zhang, T. Koschny and C. M. Soukoulis, *Advanced Optical Materials*, 2016, **4**, 1824-1828.
71. P. Zhang, N. H. Shen, T. Koschny and C. M. Soukoulis, *Acs Photonics*, 2017, **4**, 181-187.
72. Y. Fan, N.-H. Shen, F. Zhang, Q. Zhao, Z. Wei, P. Zhang, J. Dong, Q. Fu, H. Li and C. M. Soukoulis, *ACS Photonics*, 2018, **5**, 1612-1618.
73. M. J. Xia, M. Zhu, Y. C. Wang, Z. T. Song, F. Rao, L. C. Wu, Y. Cheng and S. N. Song, *Acs Appl Mater Inter*, 2015, **7**, 7627-7634.
74. M. Zhu, M. J. Xia, Z. T. Song, Y. Cheng, L. C. Wu, F. Rao, S. N. Song, M. Wang, Y. G. Lu and S. L. Feng, *Nanoscale*, 2015, **7**, 9935-9944.
75. M. Zhu, L. C. Wu, Z. T. Song, F. Rao, D. L. Cai, C. Peng, X. L. Zhou, K. Ren, S. N. Song, B. Liu and S. L. Feng, *Applied Physics Letters*, 2012, **100**, 122101.
76. M. Zhu, M. J. Xia, F. Rao, X. B. Li, L. C. Wu, X. L. Ji, S. L. Lv, Z. T. Song, S. L. Feng, H. B. Sun and S. B. Zhang, *Nature Communications*, 2014, **5**, 4086.
77. M. Zhu, L. C. Wu, F. Rao, Z. T. Song, M. J. Xia, X. L. Ji, S. L. Lv and S. L. Feng, *Applied Physics Letters*, 2014, **104**, 063105.
78. A. L. Greer and N. Mathur, *Nature*, 2005, **437**, 1246-1247.
79. B. Gholipour, J. F. Zhang, K. F. MacDonald, D. W. Hewak and N. I. Zheludev, *Advanced Materials*, 2013, **25**, 3050-3054.
80. M. L. Tseng, B. H. Chen, C. H. Chu, C. M. Chang, W. C. Lin, N. N. Chu, M. Mansuripur, A. Q. Liu and D. P. Tsai, *Optics Express*, 2011, **19**, 16975-16984.
81. M. Zhu, L. C. Wu, F. Rao, Z. T. Song, K. Ren, X. L. Ji, S. N. Song, D. N. Yao and S. L. Feng, *Applied Physics Letters*, 2014, **104**, 053119.
82. M. Zhu, O. Cojocarumirédin, A. M. Mio, J. Keutgen, M. Küpers, Y. Yu, J. Y. Cho, R. Dronskowski and M. Wuttig, *Advanced Materials*, 2018, 1706735.
83. D. E. Aspnes, *Am J Phys*, 1982, **50**, 704-709.